Transfer of 13C between paired Douglas-fir seedlings reveals plant kinship effects and uptake of exudates by ectomycorrhizas

Article

Accepted Version

Transfer of ^{13}C between paired Douglas-fir seedlings reveals plant kinship effects and uptake of exudates by ectomycorrhizas

Brian J. Pickles[1,3*], Roland Wilhelm[2*], Amanda K. Asay[1], Aria S. Hahn[2], Suzanne W. Simard[1], and William W. Mohn[2]

[1]Department of Forest and Conservation Sciences, University of British Columbia, Vancouver, BC, V6T 1Z4, Canada. [2]Department of Microbiology & Immunology, Life Sciences Institute, University of British Columbia, Vancouver, BC, V6T 1Z3, Canada. [3]School of Biological Sciences, University of Reading, Harborne Building, Whiteknights, Reading, RG6 6AS, UK

[*]These authors contributed equally to this work.

Author for correspondence:
Brian J Pickles
Tel: +44 118 378 7955
Email: b.j.pickles@reading.ac.uk

Word counts – Summary 197. Total: approx. 5030. Introduction 1027, Methods 1661, Results 1054, Discussion: 1203, Acknowledgements: 85.
Tables: 3
Figures: 4 [Colour figures: 1, 4]
Supporting information: Methods 2, Figures 6
Running title: Kinship and mycorrhizal effects on carbon transfer
Subject categories: plant-soil interactions, multi-trophic systems, mycorrhizas [Fungal paper; Plant-relevant soil processes]

Conflict of interest statement: The authors declare no conflict of interest.

Summary

- Processes governing the fixation, partitioning, and mineralization of carbon in soils are under increasing scrutiny as we develop a more comprehensive understanding of global carbon cycling. Here we examined fixation by Douglas-fir seedlings and transfer to associated ectomycorrhizal fungi, soil microbes, and full-sibling or non-sibling neighbouring seedlings.

- Stable isotope probing with 99% ^{13}C-CO_2 was applied to trace ^{13}C-labelled photosynthate throughout plants, fungi, and soil microbes in an experiment designed to assess the effect of relatedness on ^{13}C-transfer between plant pairs. The fixation and transfer of ^{13}C-label to plant, fungal, and soil microbial tissue was examined in biomass and PLFAs.

- After a 6-day chase period, approximately 26.8% of the ^{13}C remaining in the system was translocated belowground. Enrichment was proportionally greatest in ectomycorrhizal biomass. The presence of mesh barriers (0.5 or 35 μm) between seedlings did not restrict ^{13}C-transfer.

- Fungi were the primary recipients of ^{13}C-labelled photosynthate throughout the system, representing 60–70% of total ^{13}C-enriched phospholipids. Full-sibling pairs exhibited significantly greater ^{13}C-transfer to recipient roots in two of four Douglas-fir families, representing 3- and 4-fold increases (+ approx. 4 μg excess ^{13}C) compared to non-sibling pairs. The existence of a root/mycorrhizal exudation – hyphal uptake pathway was supported.

Key words (5-8): Carbon allocation / ectomycorrhizas / host relatedness / interior Douglas-fir / PLFA / stable-isotope probing.

Introduction

Accurate estimates of belowground carbon cycling are critical to linking terrestrial ecosystems with biogeochemical processes and making useful predictions about how these may change under future climates (Richter & Billings, 2015). In temperate forests, the estimated quantities of atmospheric carbon sequestered via fixation are globally-relevant (~73-159 Pg C aboveground, and 153-195 Pg C belowground; Reichstein, 2007; Lorenz & Lal, 2010), with humid and warm evergreen forests displaying the highest gross primary production of any temperate or boreal forest types (Luyssaert *et al.*, 2007). Photosynthate is mainly incorporated into plant biomass, but also supports a diverse microbial soil community either directly, via mycorrhizal fungi, or more generally, via scavenging of root exudates (Nehls *et al.*, 2007; Phillips *et al.*, 2011) and rhizodeposits (Jones *et al.*, 2009). Studying the belowground ecology governing carbon cycling is challenging due to the complexity of these communities and soil systems in general (De Deyn *et al.*, 2008; Bardgett *et al.*, 2013), and requires quantitative data on the allocation of photosynthate to plant biomass and its transfer to mycorrhizal fungi and microbes (Kaiser *et al.*, 2015). Here we undertook a multifaceted exploration of carbon allocation within and between paired interior Douglas-fir (*Pseudotsuga menziesii* var. *glauca*) seedlings, their mycorrhizal symbionts, and soil microbiota.

While the majority of plants form mycorrhizas, less than 5% of plant species are estimated to associate with ectomycorrhizal fungi (EMF). However, globally, these interactions are abundant in all forest biomes (Brundrett, 2009). Soils in ecosystems where ectomycorrhizal plants dominate exhibit higher C:N ratios compared to soils where they do not (Averill *et al.*, 2014), and ectomycorrhizal hosts have been found to allocate 10% – 30% of their photosynthate to mycorrhizas (Söderström, 1992; Leake *et al.*, 2006; Högberg & Read, 2006). EMF incorporate photosynthate into their biomass, enhancing carbon sequestration by synthesising recalcitrant carbon compounds like chitin (Clemmensen *et al.*, 2013; Kashian *et al.*, 2013), especially in poorly oxygenated soil where decomposition is slow (Wallander *et al.*, 2001). Additionally, EMF add mineral nutrients to soils through the breakdown of rock with organic acids (Hoffland *et al.*, 2003; Plassard & Fransson, 2009), and promote soil aggregate formation and carbon sequestration by exuding extracellular proteins and compounds that bind mineral particles (Rillig & Mummey, 2006; Graf & Frei, 2013). However, not all mycorrhizal activity is a carbon sink. In addition to respiration of host-derived photosynthate, some EMF species can decompose plant litter to acquire limiting nutrients, thus releasing soil carbon back into the atmosphere at rates comparable to saprotrophic fungi (Talbot *et al.*, 2008; Rineau *et al.*, 2013; Phillips *et al.*, 2014). Therefore, to assess how these processes jointly influence the

dynamics of soil carbon cycling in complex belowground systems, quantification of the fate of photosynthate in EMF-dominated systems is required.

An emergent property of mycorrhizal systems is the common mycorrhizal network, which arises when a fungal mycelium connects multiple plant hosts belowground across scales of cm^2 to at least tens of m^2 (Selosse *et al.*, 2006; Beiler *et al.*, 2010; Simard *et al.*, 2012). Ectomycorrhizal networks have been demonstrated to transfer water, nitrogen, and small quantities of carbon between interior Douglas-fir hosts (Simard *et al.*, 1997a; Teste *et al.*, 2009; Bingham & Simard, 2011). Evidence that EMF display trait heritability based on host and fungal genotype (Rosado *et al.*, 1994a,b; Karst *et al.*, 2008), and that closely related plants display greater arbuscular mycorrhizal network size and root colonisation (File *et al.*, 2012; Dudley *et al.*, 2013), raises the possibility of preferential connectivity of kin through compatibility of parent-mycorrhiza-offspring genotypes. This has not previously been explored in conifers. In arbuscular mycorrhizal grassland plant species, root exudates play a role in 'kin recognition' (Dudley *et al.*, 2013) by moderating intra- and inter-specific plant root behaviour (Semchenko *et al.*, 2014), suggesting that plant relatedness may influence nutrient uptake or transfer by altering root growth and hence mycorrhizal formation. The finding that root exudates are important in kin recognition suggests that mycorrhizas are involved in recognition mechanisms in temperate forests, where trees are comprehensively mycorrhizal. If nutrient transfer through ectomycorrhizal networks can also differ with host relatedness, then fitness, and thereby forest stand composition, may be altered (Simard, 2009). Thus, to assess the potential for host relatedness effects in the experimental system, the extent of carbon transfer between 'kin' (full sibling) and 'non-kin' (no shared parent) seedling pairs was quantified.

Although mycorrhizal fungi are known to transfer labelled carbon between plants (Finlay & Read, 1986; Simard *et al.*, 1997b), interpretations are split between those suggesting retention of labelled carbon by fungi within their biomass (Graves *et al.*, 1997; Fitter *et al.*, 1998; Wu *et al.*, 2001) and those indicating small (Simard *et al.*, 1997a; Teste *et al.*, 2010; Philip *et al.*, 2010) or large (Klein *et al.*, 2016) degrees of carbon transfer through fungal mycelium and into plant biomass. The transfer of carbon between plants may also occur via uptake of root exudates along an 'exudation-dissolved organic carbon-mycorrhizal hyphae' pathway (Robinson & Fitter, 1999), and these hypotheses regarding the mechanism of transfer need not be mutually exclusive. In this experiment we established a size-hierarchy between seedlings of different ages together in the same pot, separated by a mesh barrier to prevent direct root interaction, and labelling the larger (older) seedling with ^{13}C-CO_2.

A small number of stable isotope probing (SIP) studies, in which a plant is exposed to ^{13}C-labelled CO_2 and the distribution of ^{13}C-photosynthate is examined after a specific time period, have investigated interconnections between the Pinaceae and their EMF symbionts (see Epron *et al.*, 2012). Here, for the first time in a paired seedling model system, we investigated the fungal and microbial communities active in plant photosynthate assimilation and transfer, applying SIP methods to quantify ^{13}C allocation to plant and fungal biomass and the phospholipid fatty acids (PLFA) of plants, fungi, and bacteria (Boschker *et al.*, 1998). Our study examined paired interior Douglas-fir seedlings with the following objectives: (i) to quantify the distribution of ^{13}C-labeled photosynthate throughout plant and soil carbon pools and within microbial biomass, (ii) to determine the proportion of carbon transferred (if any) between seedlings by EMF symbionts, and (iii) to determine whether relatedness has a role in carbon transfer between conifer seedlings.

Materials and methods

Seed and soil

Seeds from four 'families' (cross-bred from four different pairs of known parents) of interior Douglas-fir (*Pseudotsuga menziesii* (Mirb.) Franco var. *glauca* (Beissn.) Franco) were sourced from the B.C. Ministry of Forests, Lands, and Natural Resource Operations (Kalamalka Research Station, B.C.). To encourage EMF colonization, seeds were grown in a soil mixture with the following specifications: 1:1 mix (approximately 3.4 L total) of autoclaved potting soil (1.7 L 1:1 mix of peat to perlite) and forest soil (1.7 L). Forest soil was classified as Dystric Brunisol (Inceptisol in U.S. soil taxonomy) with moderate humus and sandy loam texture (Soil Classification Working Group, 1998). Soil was collected from two sub-locations within a mono-specific interior Douglas-fir stand (120.58°W, 49.43°N) in the Dry, Cool Interior Douglas-fir (IDFdk) biogeoclimatic subzone (Pojar *et al.*, 1987). Following the removal of the litter layer, the fermentation layer, humus layer, and mineral soil were sampled to a total depth of 10-15 cm. Large debris was removed during collection and soil was homogenised in clean conditions before sub-sampling to create experimental units.

Experimental design and seedling growth

Each experimental unit was a 3.8 L pot containing a pair of seedlings of different ages to establish a carbon gradient, which were spaced approximately 8 cm apart and separated by a nylon mesh bag (Plastok® Meshes and Filtration Ltd., Birkenhead, UK). One 'donor' seedling was established from seed planted in March 2012 in the 805 g (11.9 s.e.m.) dry weight soil

156 outside the mesh bag. One 'recipient' seedling was established from seed planted in November
157 2012 inside the 8 x 18 cm mesh bag containing 403 g (5.9 s.e.m.) dry weight soil. Seedlings
158 were grown in a glasshouse without supplementary light or fertiliser, in order to encourage
159 mycorrhizal formation. Pots were watered to field capacity once per week following an early
160 germination period of light daily watering. A fine gravel layer was applied to soil surfaces to
161 discourage infection and mortality by pathogenic soil fungi (e.g. *Fusarium*, *Phytophthora*,
162 *Pythium*, *Rhizoctonia*; colloquially called 'damping off' fungi). Harvesting took place in the
163 first week of February 2013, when donor and recipient seedlings were 11 and 3 months old,
164 respectively (Asay, 2013).
165 Seedling relatedness was manipulated through seed origin: seedling pairs were either
166 full siblings (same parents; 'kin') or non-siblings (different parents; 'non-kin'). Kin seed was
167 obtained from four pairs of parent trees to assess whether any relatedness effects were a
168 general observation or family specific. Sufficient seed was provided to establish 10 kin pairs
169 from each of the four sets of parents (n=40). Non-kin seed was more readily available so
170 additional pairs were planted (n=60). Hyphal connection was manipulated via mesh bags:
171 seedling pairs were separated by a root-blocking barrier that either allowed the passage of EMF
172 hyphae (35 μm mesh) or was expected to restrict or prevent the passage of EMF hyphae (0.5
173 μm) (Teste *et al.* (2006). Mesh sizes were divided equally among the relatedness treatments
174 resulting in the following experimental factors: kin-unrestricted (n=20), kin-restricted (n=20),
175 non-kin-unrestricted (n=30), non-kin-restricted (n=30).
176
177 *$^{13}CO_2$ isotope labelling*
178 Donor plants were pulse-labelled with 99 atom% ^{13}C-CO_2 eleven months after they
179 were established in pots. Surviving pairs in each treatment were assigned to subsequent
180 analyses as follows. To estimate the initial uptake and fixation of ^{13}C-label, we assessed
181 incorporation of ^{13}C-photosynthate into plant and fungal biomass 1 day after labelling ("1-day
182 chase"): non-kin-unrestricted (n=3), non-kin-restricted (n=3), non-labelled controls (n=3). To
183 examine the transfer and incorporation of ^{13}C-photosynthate into biomass 6 days after labelling
184 ("6-day chase"): kin-unrestricted (n=9), kin-restricted (n=8), non-kin-unrestricted (n=10), non-
185 kin-restricted (n=10). Unlabelled controls consisted of kin-unrestricted (n=9), kin-restricted
186 (n=8), non-kin-unrestricted (n=7), non-kin-restricted (n=7).
187 Immediately before labelling, all donor seedlings were sealed using Tuck® Contractors
188 Sheathing Tape inside plastic Foodsaver® vacuum bags (6 L). Bags were fitted with an
189 injection valve and inflated with ambient air. Non-labelled control seedlings were bagged in

the same manner and stored with a minimum separation distance of 4 m from the nearest labelled seedling. Three injections of ^{13}C-CO_2 were received by labelled seedlings at equal time intervals through the 10 h pulse period, totalling 50 mL of ^{13}C-CO_2 (with maximum concentrations of 2500-3000 ppm). An additional seedling was used to monitor bag CO_2 concentration using a portable infrared gas analyser (Qubit Systems, Kingston, Canada). Ambient greenhouse CO_2 levels (394 ppm) were checked prior to labelling, 5 h after labelling, and 10 h after labelling and showed no significant variation. After the final pulse, when bag CO_2 concentrations had dropped below 300 ppm, labelling bags were removed.

Sampling of plant and soil pools

Eleven distinct plant and soil pools were examined in this experiment, with donor (D) and recipient (R) seedling samples collected as described in Figure 1. Due to growth stage differences between donor and recipient seedlings, root sections were collected from donor transport fine roots (McCormack *et al.*, 2015) and the recipient's main tap root, which were of equivalent diameter and structure (i.e. no absorptive fine roots were included in these samples). Samples were kept on dry ice after weighing, and stored at -80 ^{o}C. All fine root tips were sampled from each seedling, morphotyped based on ectomycorrhizal structures or their absence (Goodman *et al.*, 1998), then counted and weighed prior to subsampling for fungal identification via amplified internal transcribed spacer (ITS) sequences. All root tips from six plant pairs were kept on dry ice after weighing, and stored at -80 ^{o}C. Soil for PLFA analyses was immediately frozen in liquid nitrogen before storage at -80 ^{o}C. Samples were lyophilized prior to DNA or PLFA extraction and isotopic analysis. Remaining plant biomass from each pool was oven-dried and weighed.

Isotopic measurements

Total carbon and nitrogen content and carbon isotopic composition of samples were measured with combustion analysis using an elemental analyzer (Elementar, Hanau, Germany) in C, N mode, interfaced with an isotope-ratio mass spectrometer (IRMS; Isoprime, Cheadle, UK). Samples were considered enriched if their $\delta^{13}C$ value was greater than the upper 99% confidence interval of the control mean $\delta^{13}C$ (natural abundance) and all control sample $\delta^{13}C$ values. Atom $\%^{13}C$ excess was calculated for each pool as per Leake *et al.* (2006). Teste *et al.*'s (2009) modification of Boutton's (1991) isotopic calculations was applied to convert $\delta^{13}C$ into "excess ^{13}C" as ^{12}C-equivalent (mg), the mass of labelled carbon compensating for the one Dalton difference in mass of ^{12}C.

Isotopic composition of PLFAs was analysed using gas chromatography-IRMS, following extraction according to Bligh & Dyer (1959), as detailed in Churchland *et al.* (2013), with the following exceptions: (i) methyl undecanoate (c11:0) was the internal standard, and (ii) quantitation was performed based on average values derived from serial dilution of undecanoate, nonadecanoate (c19:0), and methyl cis-13-docosenoate (c22:1ω9). Peak identification was based on retention time compared to two reference standards: bacterial acid methyl-ester standard 47080-0 (Sigma–Aldrich, St. Louis, USA) and a 37-Component fatty acid methyl-ester mix (47885-U). Unidentifiable ^{13}C-enriched peaks were included in analysis if they met the following conditions: i) detection in > 3 samples, ii) average $\delta^{13}C > +50$ ‰. Taxonomic affiliations of specific PLFAs were assigned as per Högberg *et al.* (2013), with c18:1ω9 and c18:3ω6 added as fungal markers, according to Ruess & Chamberlain (2010).

Fine root tip fungal DNA extraction-sequencing

Fungal DNA was extracted from multiple representative root tips of each EMF morphotype, from which adhering soil had been carefully removed, using ITS1 (White *et al.*, 1990) and ITS4/ITS4B primers (Gardes & Bruns, 1993) following the protocol provided in Supporting Methods S1. Raw sequence data were analysed using SEQUENCHER Version 3.0 (Gene Codes Corp., Ann Arbor, USA) and converted into FASTA format prior to comparison with the UNITE database (Kõljalg *et al.*, 2013), using the BLAST algorithm to identify each fungal species. Sequence data were deposited in the GenBank database as accession numbers KT314836 to KT314861. Three samples from the rhizosphere soil partition were selected for metatranscriptomic sequencing to assess activity of root-associated communities (Supporting Methods S2).

Statistical analyses

All analyses were performed using R 3.2.3 (R Core Team, 2015) unless otherwise stated. Data was square root or $\log_{10}$ transformed where necessary to meet parametric assumptions, with highly influential data points ($\geq$ 3 st. dev. from the treatment median) treated as statistical outliers and removed prior to analysis. Differences between treatments in the excess ^{13}C content of recipient pools were assessed by fitting linear mixed models in R-packages "nlme" (Pinheiro *et al.*, 2016) and "lme4" (Bates *et al.*, 2015). The fixed factors in each model were: seedling relatedness (kin or non-kin), hyphal restriction (35 µm or 0.5 µm), recipient family (A, B, C, or D), and their two-way interactions. In all models, donor family was included as a random factor. The response variables examined were "excess ^{13}C as ^{12}C

equivalent" of the R_{bulk}, $R_{rhizosphere}$, R_{ECM}, and R_{root} pools. Model fit was determined using R-package "piecewiseSEM" (Lefcheck, 2016). Standardised coefficients, a measure of standardised effect size (SES) (Schielzeth, 2010), were estimated for each model (regression coefficients divided by two times their standard deviation).

Linear models were used to assess whether excess ^{13}C in kin and non-kin recipient pools displayed different relationships to potentially explanatory biological factors (D_{shoot} ^{13}C-enrichment, D_{ECM} ^{13}C-enrichment, D_{ECM} abundance). SES was measured using Cohen's *d* (Cohen, 1988). False discovery rate (FDR) correction (Verhoeven *et al.*, 2005) was applied where data was regressed against multiple factors.

Enriched fungal biomass (^{13}C per g tissue dry weight) was calculated by converting from mg enriched fungal PLFAs, using the conversion factor provided by Joergensen & Wichern (2008). Average carbon incorporation into fungal biomass was calculated for D_{ECM} (reflecting the hartig net, mantle, and extramatrical mycelium of EMF) and D_{root} (to account for the presence of fungal endophytes and any potential extension of EMF hyphae into transport fine roots; see Kaiser et al., 2010).

Seedling EMF community data was examined with the Sørensen (Bray-Curtis) distance measure using nonparametric multi-dimensional scaling (NMDS) and multi-response permutation procedures (MRPP) in PC-Ord 5 (MjM Software, Gleneden Beach, USA).

All data used in this analysis, along with a custom script for processing SIP-PLFA data, can be found at the stable URL: https://github.com/roli-wilhelm.

Results

Partitioning of ^{13}C-labeled photosynthate

Every plant and soil pool exhibited elevated levels of ^{13}C-labelled carbon relative to the natural abundance in unlabelled controls (Table 1). No significant differences in $\delta^{13}C$ were observed among unlabelled controls. ^{13}C-enrichment of R_{shoot}, the most distant pool from donor plants, was significant in 4 kin and 2 non-kin samples (6/37). The decrease in ^{13}C-labelled carbon, from D_{shoot} to R_{shoot}, revealed the scope and scale of carbon flow through the belowground system (Table 1; Supplementary Figure S1a). As expected, in each plant D_{ECM} and R_{ECM} contained significantly more ^{13}C-labelled carbon as a percentage of their total carbon content compared to all other pools, illustrating their assimilation of this carbon (Supplementary Figure S1b).

Of the total mass of pulsed ^{13}C-labelled carbon (29.02 mg), approximately 75.4% (21.88 mg) was fixed in donor plant tissue after the 1-day chase. Following the 6-day chase

period, approximately 44.1% (9.64 mg) of the fixed label (33.2% of the pulse) was detected across all biomass pools. The total transfer to measured belowground and recipient pools was approximately 12% of the ^{13}C-label fixed, amounting to 26.8% of the total ^{13}C-label detected in the 6-day chase. For an account of all individual pools see Table 1. The remaining unaccounted ^{13}C-label was either not fixed or fixed and respired during the labelling period.

A strong inverse relationship was observed between D_{shoot} δ^{13}C and donor biomass (r^2 = 0.66, $P < 0.001$), while the total mass of excess ^{13}C in D_{shoot} did not vary significantly with donor biomass ($r^2 < 0.01$, $P = 0.29$). Thus larger plants had a lower ^{13}C-content relative to total seedling biomass than smaller plants.

Role of seedling relatedness and ectomycorrhizal hyphae in carbon transfer

Analysis using linear mixed models revealed a seedling relatedness effect on R_{root} excess ^{13}C, with the significant model interaction term revealing variation between the four recipient families (Table 2). Significantly greater R_{root} excess ^{13}C was observed in kin recipients from families A and B than in non-kin recipients (Fig. 2a), whereas there was no significant difference based on relatedness in families C and D. In terms of µg excess ^{13}C this represented a 3-fold increase in kin of family A (kin mean 5.7 µg; non-kin mean 1.9 µg), and a 4-fold increase in kin of family B (kin mean 5.6 µg; non-kin mean 1.4 µg). Carbon transfer to other recipient pools was not significantly different between relatedness treatments (Table 2). Linear regression analysis revealed that R_{root} δ^{13}C enrichment increased with increasing D_{ECM} abundance in kin pairs only (Fig. 3a). In both kin and non-kin pairs, R_{bulk} δ^{13}C enrichment increased with increasing D_{ECM} abundance (both: $r^2 = 0.34$, kin: $P = 0.014$; non-kin: P = 0.007). In kin pairs only, R_{ECM} excess ^{13}C was positively associated with that of both D_{ECM} (Fig. 3b) and D_{shoot} (Fig. 3c).

Hyphal exclusion did not reduce colonisation of recipient roots, or significantly reduce overall sub-surface carbon transfer. However, analysis using linear mixed models (Table 2) indicated a reduction in R_{bulk} excess ^{13}C with hyphal exclusion in recipient family D (SES = 0.60-0.66), and reduced $R_{rhizosphere}$ excess ^{13}C among kin recipients in families C (SES = 0.58) and D (SES = 0.62). Conversely, increased R_{root} excess ^{13}C with hyphal exclusion was observed for kin in recipient family A and regardless of relatedness in family D (Fig. 2b). Carbon transfer to other recipient pools did not differ between mesh treatments (Table 2).

To assess whether the observed relatedness effects could be due to differences in belowground biomass allocation between families, the same linear mixed models were performed for donor and recipient root: shoot ratio, and the biomass of D_{root}, R_{root}, D_{ECM} and

R_{ECM}. The only significant factor across these models was that family C exhibited a lower root: shoot ratio than the other three families. No other fixed or interactive factors proved to be significant (data not shown).

Assimilation of ^{13}C-photosynthate by the microbial community

Total ^{13}C-incorporation into PLFAs in all pools amounted to 1% of belowground carbon transfer (0.023 mg ^{13}C in PLFAs / 2.31 mg total ^{13}C transferred). Fungal PLFA ^{13}C-enrichment was 5.57 mg fungal C g^{-1} dry weight in D_{ECM} and 1.97 mg fungal C g^{-1} dry weight in D_{root}. Estimated D_{ECM} PLFA ^{13}C-enrichment was strongly correlated with ^{13}C-enrichment of D_{ECM} tissue ($r^2 = 0.844$, $P < 0.001$), and D_{ECM} PLFAs contained the highest total excess ^{13}C measured (Supplementary Figure S2). The D_{root} pool contained the next highest level of PLFA ^{13}C-enrichment, originating from the plant root and associated fungi and bacteria. Fungal PLFA markers were the most ^{13}C-enriched in all pools, containing ~70% of assimilated ^{13}C-label. The second most ^{13}C-enriched taxonomic group were the 'higher eukaryotes,' a heterogeneous category of long-chain fatty acids, indistinguishable between fungi, plants, and other eukaryotic species.

Microbes closely associated with host roots were less diverse than those in soil (~27 PLFAs), based on the average number of enriched PLFAs (D_{root}: 12, D_{ECM}: 9, R_{ECM}: 13). Differences between root-associated and soil-associated communities were evident in ^{13}C-enriched PLFA profiles (Supplementary Figure S3) and unidentified fatty acid profiles (Supplementary Figure S4). The D_{coarse} community was the most distinct, displaying increased ^{13}C-enrichment of medium-length fatty acids between c14:0 – c16:1ω9. Fungi assimilated the vast majority of photosynthate based on total ^{13}C-enrichment of PLFAs; however, other taxonomic groups in the rhizosphere exhibited substantial assimilation rates (Fig. 4). In the D_{root} pool bacteria incorporated ^{13}C-label at rates comparable to that of fungi (i.e. relative to their biomass). Gram-negative bacteria assimilated significant amounts of ^{13}C-exudate across all donor pools in every sample assayed, whereas gram-positive bacteria did not assimilate detectable ^{13}C-exudate in ectomycorrhizal pools.

Fungal root-tip community

Seedlings were primarily colonised by *Rhizopogon vinicolor*, and an ectomycorrhizal Pyronemataceae sp. (Table 3), both of which were also detected in a preliminary metatranscriptomic analysis of three rhizosphere soil samples (Supporting Methods S1 and Fig. S5). The abundance of these EMF species on recipient seedlings was positively related to their

abundance on donor seedlings regardless of treatment. MRPP analysis following NMDS ordination (Supporting Fig. S6) revealed that the only significant difference between EMF communities was weak and occurred between donor and recipient seedlings, rather than treatments ($A = 0.131$, $P < 0.001$; where $A > 0.3$ is considered an ecologically relevant effect). Notably, in the sole case where a plant lacked *Rhizopogon* sp. ectomycorrhizas, ^{13}C-enrichment was not detected in recipient pools.

Discussion

Fungi dominated the assimilation of photosynthetic carbon in all belowground experimental pools, with ectomycorrhizal fungi serving as major agents of carbon transfer. EMF incorporation of photosynthate from host plants is hypothesised to be a major factor in carbon sequestration in coniferous forests (Clemmensen *et al.*, 2013). An estimated 26.8% of the ^{13}C-label remaining in the system was recovered from belowground pools (primarily donor roots), of which 6.3% was assimilated by, or transferred through, EMF. Carbon transfer from donor to recipient seedlings was significantly greater to sibling roots than non-sibling roots in two of the Douglas-fir families, indicating a host relatedness effect that was most likely mediated by EMF. The transfer of ^{13}C-label in the presence of a hyphae-restricting mesh implies that labile ^{13}C-compounds were exuded into soil by donor roots and/or EMF, before being taken up by recipient hyphae. Overall we observed that a diverse microbial community was actively assimilating ^{13}C-labeled photosynthate.

Scale and significance of belowground partitioning of Douglas-fir photosynthate

Carbon allocation to donor plant root and ectomycorrhzial root tip biomass (~23% of the total recovered) was within the range of previously estimated allocation values for ectomycorrhizal seedlings of other species: Norway spruce, Scots pine, and silver birch (13-24%; Pumpanen *et al.*, 2008), Scots pine (31%; Heinonsalo *et al.*, 2010), and willow (47%; Durall *et al.*, 1994). Furthermore, ^{13}C-enrichment of fungal-specific PLFAs indicated significant carbon allocation to fungi within donor transport fine roots, most likely attributable to intra-root EMF biomass (Kaiser *et al.*, 2010) and/or fungal endophytes.

Mycorrhizal networks in mature forests can be extensive (Beiler *et al.*, 2010), offering the potential for substantial carbon transfer among plants. Yet the net benefit of seedling-to-seedling carbon transfer remains poorly understood. Previous research indicates that EMF and their mycorrhizal networks mediate the transfer of variable amounts of carbon (Simard *et al.*, 1997a; Teste *et al.*, 2009; Philip *et al.*, 2010), water (Allen, 2007; Plamboeck *et al.*, 2007;

Bingham & Simard, 2011), and nitrogen (He *et al.*, 2003; Read & Perez-Moreno, 2003; Teste *et al.*, 2009) between plants. The quantities of seedling-seedling carbon transfer measured in our experiment (~0.1% of total recovered ^{13}C-label across all pools) and elsewhere (Teste *et al.*, 2009, 2010) are small, and unlikely to represent a substantial nutritional source. However, research on the EMF host-symbiont interface reveals that EMF produce signalling compounds, which are translocated into plant cell nuclei. For example, *Laccaria bicolor* produces the MiSSP7 protein, which alters the host transcriptome to promote ectomycorrhizal formation and reduce jasmonic acid production (Plett *et al.*, 2011, 2014). Our observations may therefore represent the transfer of signalling compounds through a fungal mycelium, or their uptake by roots or fungal hyphae following exudation. The stimulation of physiological responses in recipient plants by potential signalling compounds has previously been observed in arbuscular mycorrhizal systems (Babikova *et al.*, 2013; Song *et al.*, 2014) and EMF systems involving interior Douglas-fir and ponderosa pine (Song *et al.*, 2015).

Host relatedness

Intriguingly, kin pairs exhibited increased carbon transfer to the R_{root} pool in two of the four Douglas-fir families, with excess ^{13}C in those families 3 to 4-fold greater than in non-kin pairings. The absolute quantities of increased excess ^{13}C involved in this relatedness effect were small (+ 4 μg), but represented a large proportion of total recipient plant excess ^{13}C content (overall recipient plant mean: 6.4 μg). The strong positive relationship between R_{root} δ^{13}C and D_{ECM} abundance in kin pairs demonstrated that the genetic relatedness effect on carbon transfer involved donor plant EMF. This was further reinforced by the positive relationships between excess ^{13}C in the R_{ECM} pool and both the D_{shoot} and D_{ECM} pools in kin pairs. Further investigation is required, but we propose that the establishment of an ectomycorrhizal symbiosis between an individual fungal mycelium and a host plant may increase both the likelihood that the fungus will successfully colonise other hosts of a similar genotype, and the efficiency of carbon transfer through its mycelium. In our system, *Rhizopogon* spp. and the ectomycorrhizal Pyronemataceae sp. are the most likely candidate fungi due to their abundance on seedling roots and their detected activity in soil metatranscriptomes. We further hypothesise that increased carbon transfer among kin seedlings may have resulted from (i) increased inter-root EMF biomass between compatible host genotypes (Rosado *et al.*, 1994a,b; Dudley *et al.*, 2013), and/or (ii) increased inter-root activity due to increased transfer of signalling compounds and/or micronutrients (Plett *et al.*, 2011; Babikova *et al.*, 2013). Alternative explanations for the observed carbon transfer are

certainly possible, but would have to account for the significant interaction between relatedness and family (e.g., differences in belowground carbon allocation between families would not explain why increased transfer of ^{13}C to roots in families A and B only occurred in the presence of kin).

Hyphal restriction

Transfer of ^{13}C-carbon to recipient pools occurred regardless of hyphal exclusion, demonstrating that ^{13}C-compounds can be transferred in the absence of a direct linkage between mycorrhizal hyphae (e.g. Robinson & Fitter, 1999). Carbon transfer was clearly associated with mycorrhizas, since: (i) exclusion reduced transfer to bulk soil in some of the recipient families; (ii) donor and recipient EMF abundance was positively associated for several EMF species; (iii) D_{ECM} abundance was associated with enrichment of recipient pools; and (iv) D_{ECM} and R_{ECM} biomass contained proportionally more ^{13}C-label than all other pools. Previous studies similarly reported small quantities of ^{13}C transfer across a 0.5 μm mesh in both ectomycorrhizal (Teste *et al.*, 2009; Philip *et al.*, 2010; Deslippe & Simard, 2011) and arbuscular mycorrhizal (Fitter *et al.*, 1998) systems. Thus, the mesh-bagging treatment may not be effective for preventing mycorrhizal-mediated carbon transfer. This is potentially due to: (i) recipient EMF hyphae scavenging donor ^{13}C-exudates that diffused through the mesh (Robinson & Fitter, 1999; Johnson & Gilbert, 2015), (ii) hyphae fusing across the mesh, or (iii) hyphae breaching the mesh, possibly degrading it via secreted organic acids (Plassard & Fransson, 2009). No breaches were observed in our experiment, but consistent with possibilities (i) and (ii), there were regions of mesh with adjacent patches of hyphae on either side. Future experiments could employ the in-growth core rotation method (Johnson *et al.*, 2001) to reduce the possibility of (ii) and (iii), although it is unlikely to prevent (i), which represents an alternative belowground transfer pathway in natural systems (Simard et al. 1997b; Robinson & Fitter, 1999; Philip *et al.*, 2010; Deslippe & Simard, 2011).

Conclusions

Our stable isotope approach successfully elucidated the pattern and scale of mycorrhiza-mediated carbon transfer between interior Douglas-fir seedlings, and the incorporation of enriched carbon into microbial biomass. EMF symbionts, specifically *Rhizopogon* spp. and Pyronemataceae sp., were the primary external beneficiaries of host-derived photosynthate, and were able to take it up despite the presence of a hyphae-restricting mesh. The small quantities of carbon transferred between seedlings suggest that it is unlikely

to be an important nutritional source, although the timing and transfer of micronutrients or signalling compounds may have a substantial ecological impact. We report evidence that relatedness influences carbon transfer between donor and recipient plants, and that the presence of this effect varied between families, raising the possibility of a mosaic of relatedness effects at larger scales. These findings require further exploration in the field, however, the implications for forest ecology are substantial.

Conflict of interest statement

The authors declare no conflict of interest.

Acknowledgements

We thank Melissa Dergousoff and Scott Besse for sustained lab assistance, and Matthew Zustovic, Aaron Zwiebel, Hilary Leung, and Julia Maddison for lab and greenhouse contributions; Alice Chang provided advice on EA-IRMS analysis; Spencer Reitenbach provided the seeds used in this experiment. We also thank Ian Dickie and three anonymous referees for their comments on an earlier version of this manuscript. This project was funded by an NSERC Strategic Project grant, with individual support provided to A.S.H., R.W., and A.K.A., by NSERC and UBC scholarships.

Author contributions

A.K.A. and S.W.S. planned the seedling kin-recognition experiment, which A.K.A. performed. B.J.P., R.W., and S.W.S. designed the SIP experiment, with B.J.P. analysing the excess ^{13}C data and implementing all experimental models, and R.W. analysing the $\delta^{13}C$ data. R.W. and W.W.M. planned the analysis of ^{13}C-labelled PLFA, which R.W. performed and analysed. B.J.P. and A.K.A. collected the EMF colonisation data, which B.J.P. analysed. A.S.H. generated the metatranscriptome data, which A.S.H. and R.W. analysed. A.K.A., B.J.P., R.W., and A.S.H. performed the experiments. B.J.P. led the writing of the manuscript with significant contributions from R.W. All authors reviewed and commented on the manuscript.

Supporting Information

Additional supporting information may be found in the online version of this article.

Supporting Methods S1. EMF DNA extraction and Sanger sequencing details.

Supporting Methods S2. Metatranscriptome analysis extraction-sequencing details.

Supporting Figure S1. Boxplots of excess ^{13}C; a) biomass, b) proportion.

Supporting Figure S2. Incorporation of ^{13}C-label by microbial groups.

Supporting Figure S3. PLFA profiles of root and soil pools.

Supporting Figure S4. Profiles of unidentified PLFAs in root and soil pools.

Supporting Figure S5. Metatranscriptomic data based on Silva taxonomy.

Supporting Figure S6. NMDS ordination of seedling root tip fungal communities.

References

Allen MF. **2007**. Mycorrhizal Fungi: Highways for Water and Nutrients in Arid Soils. *Vadose Zone Journal* **6**: 291–297.

Asay AK. **2013**. Mycorrhizal facilitation of kin recognition in interior Douglas-fir (*Pseudotsuga menziesii* var. *glauca*). M.Sc. Thesis. University of British Columbia, Vancouver, BC, Canada.

Averill C, Turner BL, Finzi AC. **2014**. Mycorrhiza-mediated competition between plants and decomposers drives soil carbon storage. *Nature* **505**: 543–545.

Babikova Z, Gilbert L, Bruce T, Birkett M, Caulfield J, Woodcock C, Pickett J, Johnson D. **2013**. Underground signals carried through common mycelial networks warn neighbouring plants of aphid attack. *Ecology Letters* **16**: 835–843.

Bardgett RD, Manning P, Morrien E, De Vries FT. **2013**. Hierarchical responses of plant – soil interactions to climate change : consequences for the global carbon cycle. *Journal of Ecology* **101**: 334–343.

Bates D, Mächler M, Bolker B, Walker S. **2015**. Fitting Linear Mixed-Effects Models Using lme4. *Journal of Statistical Software* **67**: 1–48.

Beiler KJ, Durall DM, Simard SW, Maxwell SA, Kretzer AM. **2010**. Architecture of the wood-wide web: *Rhizopogon* spp. genets link multiple Douglas-fir cohorts. *New Phytologist* **185**: 543–553.

Bingham MA, Simard SW. **2011**. Do mycorrhizal network benefits to survival and growth of interior Douglas-fir seedlings increase with soil moisture stress? *Ecology and Evolution* **1**: 306–316.

Bligh E, Dyer W. **1959**. A rapid method of total lipid extraction and purification. *Canadian Journal of Biochemistry and Physics* **37**: 911–917.

Boschker HTS, Nold SC, Wellsbury P, Bos D, de Graaf W, Pel R, Parkes RJ, Cappenberg TE. **1998**. Direct linking of microbial populations to specific biogeochemical processes by ^{13}C-labelling of biomarkers. *Nature* **392**: 801–805.

Boutton T. **1991**. Stable carbon isotope ratios of natural materials: I. sample preparation and

mass spectrometric analysis. In: Coleman DC, Fry B, eds. Carbon isotope techniques. San Diego: Academic Press, 155–171.

Brundrett MC. **2009**. Mycorrhizal associations and other means of nutrition of vascular plants: Understanding the global diversity of host plants by resolving conflicting information and developing reliable means of diagnosis. *Plant and Soil* **320**: 37–77.

Churchland C, Grayston SJ, Bengtson P. **2013**. Spatial variability of soil fungal and bacterial abundance: Consequences for carbon turnover along a transition from a forested to clear-cut site. *Soil Biology and Biochemistry* **63**: 5–13.

Clemmensen KE, Bahr A, Ovaskainen O, Dahlberg A, Ekblad A, Wallander H, Stenlid J, Finlay RD, Wardle DA, Lindahl BD. **2013**. Roots and Associated Fungi Drive Long-Term Carbon Sequestration in Boreal Forest. *Science* **339**: 1615–1618.

Cohen J. **1988**. *Statistical power analysis for the behavioral sciences*. Hillsdale, NJ, USA: Lawrence Earlbaum Associates.

Deslippe JR, Simard SW. **2011**. Below-ground carbon transfer among *Betula nana* may increase with warming in Arctic tundra. *New Phytologist* **192**: 689–698.

De Deyn GB, Cornelissen JHC, Bardgett RD. **2008**. Plant functional traits and soil carbon sequestration in contrasting biomes. *Ecology Letters* **11**: 516–531.

Dudley SA, Murphy GP, File AL. **2013**. Kin recognition and competition in plants. *Functional Ecology* **27**: 898–906.

Durall D, Jones MD, Tinker PB. **1994**. Allocation of ^{14}C-Carbon in ectomycorrhizal willow. *New Phytologist* **128**: 109–114.

Epron D, Bahn M, Derrien D, Lattanzi FA, Pumpanen J, Gessler A, Högberg P, Maillard P, Dannoura M, Gérant D, *et al.* 2012. Pulse-labelling trees to study carbon allocation dynamics: a review of methods, current knowledge and future prospects. *Tree Physiology* **32**: 776–798.

File AL, Klironomos J, Maherali H, Dudley SA. **2012**. Plant Kin Recognition Enhances Abundance of Symbiotic Microbial Partner. *PLoS ONE* **7**: 15–17.

Finlay RD, Read DJ. **1986**. The Structure and Function of the Vegetative Mycelium of Ectomycorrhizal Plants . I . Translocation of ^{14}C-Labelled Carbon Between Plants Interconnected by a Common Mycelium. *New Phytologist* **103**: 143–156.

Fitter AH, Graves JD, Watkins NK, Robinson D, Scrimgeour C. **1998**. Carbon transfer between plants and its control in networks of arbuscular mycorrhizas. *Functional Ecology* **12**: 406–412.

Gardes M, Bruns TD. **1993**. ITS primers with enhanced specificity for basidiomycetes-

564 application to the identification of mycorrhizae and rusts. *Molecular Ecology* **2**: 113–118.
565 **Goodman D, Durall D, Trofymow T, Berch SM**. **1998**. A manual of concise descriptions of
566 North American ectomycorrhizae. *Mycorrhiza* **8**: 57–59.
567 **Graf F, Frei M**. **2013**. Soil aggregate stability related to soil density, root length, and
568 mycorrhiza using site-specific *Alnus incana* and *Melanogaster variegatus* s.l. *Ecological*
569 *Engineering* **57**: 314–323.
570 **Graves JD, Watkins NK, Fitter AH, Robinson D, Scrimgeour C**. **1997**. Intraspecific
571 transfer of carbon betwen plants linked by a common mycorrhial network. *Plant and Soil* **192**:
572 153–159.
573 **He X-H, Critchley C, Bledsoe C**. **2003**. Nitrogen Transfer Within and Between Plants
574 Through Common Mycorrhizal Networks (CMNs). *Critical Reviews in Plant Sciences* **22**:
575 531–567.
576 **Heinonsalo J, Pumpanen J, Rasilo T, Hurme K-R, Ilvesniemi H**. **2010**. Carbon partitioning
577 in ectomycorrhizal Scots pine seedlings. *Soil Biology and Biochemistry* **42**: 1614–1623.
578 **Hoffland E, Giesler R, Jongmans AG, Van Breemen N**. **2003**. Feldspar Tunneling by Fungi
579 along Natural Productivity Gradients. *Ecosystems* **6**: 739–746.
580 **Högberg M, Högbom L, Kleja D**. **2013**. Soil microbial community indices as predictors of
581 soil solution chemistry and N leaching in *Picea abies* (L.) Karst. Forests in S. Sweden. *Plant*
582 *and Soil* **372**: 507–522.
583 **Högberg P, Read DJ**. **2006**. Towards a more plant physiological perspective on soil ecology.
584 *Trends in ecology & evolution* **21**: 548–54.
585 **Joergensen RG, Wichern F**. **2008**. Quantitative assessment of the fungal contribution to
586 microbial tissue in soil. *Soil Biology and Biochemistry* **40**: 2977–2991.
587 **Johnson D, Gilbert L**. **2015**. Interplant signalling through hyphal networks. *New Phytologist*
588 **205**: 1448–1453.
589 **Johnson D, Leake J, Read D**. **2001**. Novel in-growth core system enables functional studies
590 of grassland mycorrhizal mycelial networks. *New Phytologist* **152**: 555–562.
591 **Jones DL, Nguyen C, Finlay RD**. **2009**. Carbon flow in the rhizosphere: carbon trading at the
592 soil–root interface. *Plant and Soil* **321**: 5–33.
593 **Kaiser C, Frank A, Wild B, Koranda M, Richter A**. **2010**. Negligible contribution from
594 roots to soil-borne phospholipid fatty acid fungal biomarkers 18:2ω6,9 and 18:1ω9. *Soil*
595 *Biology & Biochemistry* **42**: 1650–1652.
596 **Kaiser C, Kilburn MR, Clode PL, Fuchslueger L, Koranda M, Cliff JB, Solaiman ZM,**
597 **Murphy D V. 2015**. Exploring the transfer of recent plant photosynthates to soil microbes:

598 Mycorrhizal pathway vs direct root exudation. *New Phytologist* **205**: 1537–1551.
599 **Karst J, Jones MD, Turkington R**. **2008**. Ectomycorrhizal colonization and intraspecific
600 variation in growth responses of lodgepole pine. *Plant Ecology* **200**: 161–165.
601 **Kashian D, Romme W, Tinker D, Turner M, Ryan M**. **2013**. Postfire changes in forest
602 carbon storage over a 300-year chronosequence of *Pinus contorta*-dominated forests.
603 *Ecological Monographs* **83**: 49–66.
604 **Klein T, Siegwolf RTW, Korner C**. **2016**. Belowground carbon trade among tall trees in a
605 temperate forest. *Science* **352**: 342–344.
606 **Kõljalg U, Nilsson RH, Abarenkov K, Tedersoo L, Taylor A, Bahram M, Al E**. **2013**.
607 Towards a unified paradigm for sequence-based identification of fungi. *Molecular Ecology* **22**:
608 5271–5277.
609 **Leake JR, Ostle NJ, Rangel-Castro JI, Johnson D**. **2006**. Carbon fluxes from plants through
610 soil organisms determined by field $^{13}CO_2$ pulse-labelling in an upland grassland. *Applied Soil*
611 *Ecology* **33**: 152–175.
612 **Lefcheck JS**. **2016**. piecewiseSEM: Piecewise structural equation modelling in R for ecology,
613 evolution, and systematics. *Methods in Ecology and Evolution* **7**: 573–579.
614 **Lorenz K, Lal R**. **2010**. *Carbon Sequestration in Forest Ecosystems*. New York: Springer
615 New York.
616 **Luyssaert S, Inglima I, Jung M, Richardson AD, Reichstein M, Papale D, Piao SL,**
617 **Schulze ED, Wingate L, Matteucci G, *et al.* 2007**. CO_2 balance of boreal, temperate, and
618 tropical forests derived from a global database. *Global Change Biology* **13**: 2509–2537.
619 **McCormack ML, Dickie IA, Eissenstat DM, Fahey TJ, Fernandez CW, Guo D,**
620 **Helmisaari H-S, Hobbie EA, Iversen CM, Jackson RB, *et al.* 2015**. Redefining fine roots
621 improves understanding of below-ground contributions to terrestrial biosphere processes. *New*
622 *Phytologist* **207**: 505–518.
623 **Nehls U, Grunze N, Willmann M, Reich M, Kuster H**. **2007**. Sugar for my honey:
624 Carbohydrate partitioning in ectomycorrhizal symbiosis. *Phytochemistry* **68**: 82–91.
625 **Philip L, Simard S, Jones M**. **2010**. Pathways for below-ground carbon transfer between
626 paper birch and Douglas-fir seedlings. *Plant Ecology & Diversity* **3**: 221–233.
627 **Phillips RP, Finzi AC, Bernhardt ES**. **2011**. Enhanced root exudation induces microbial
628 feedbacks to N cycling in a pine forest under long-term CO_2 fumigation. *Ecology Letters* **14**:
629 187–194.
630 **Phillips LA, Ward V, Jones MD**. **2014**. Ectomycorrhizal fungi contribute to soil organic
631 matter cycling in sub-boreal forests. *The ISME journal* **8**: 699–713.

Pinheiro J, Bates D, DebRoy S, Sarkar D, Team RC. **2016**. nlme: Linear and Nonlinear Mixed Effects Models. : R package version 3.1–128, http://cran.r–project.o.

Plamboeck AH, Dawson TE, Egerton-Warburton LM, North M, Bruns TD, Querejeta JI. **2007**. Water transfer via ectomycorrhizal fungal hyphae to conifer seedlings. *Mycorrhiza* **17**: 439–447.

Plassard C, Fransson P. **2009**. Regulation of low-molecular weight organic acid production in fungi. *Fungal Biology Reviews* **23**: 30–39.

Plett JM, Daguerre Y, Wittulsky S, Vayssieres A, Deveau A, Melton SJ, Kohler A, Morrell-Falvey JL, Brun A, Veneault-Fourrey C, *et al.* 2014. Effector MiSSP7 of the mutualistic fungus *Laccaria bicolor* stabilizes the *Populus* JAZ6 protein and represses jasmonic acid (JA) responsive genes. *Proceedings of the National Academy of Sciences* **111**: 8299–8304.

Plett JM, Kemppainen M, Kale SD, Kohler A, Legué V, Brun A, Tyler BM, Pardo AG, Martin F. **2011**. A Secreted Effector Protein of *Laccaria bicolor* Is Required for Symbiosis Development. *Current Biology* **21**: 1197–1203.

Pojar J, Klinka K, Meidinger D. **1987**. Biogeoclimatic ecosystem classification in British Columbia. *Forest Ecology and Management* **22**: 119–154.

Pumpanen JS, Heinonsalo J, Rasilo T, Hurme K-R, Ilvesniemi H. **2009**. Carbon balance and allocation of assimilated CO_2 in Scots pine, Norway spruce, and Silver birch seedlings determined with gas exchange measurements and 14C pulse labelling. *Trees* **23**: 611–621.

R Core Team. **2015**. R: a language and environment for statistical computing (H Fehske, R Schneider, and A Weiße, Eds.). *R Foundation for Statistical Computing*: 409pp URL http://www.R–project.org/.

Read DJ, Perez-Moreno J. **2003**. Mycorrhizas and nutrient cycling in ecosystems - a journey towards relevance? *New Phytologist* **157**: 475–492.

Reichstein M. **2007**. Impacts of climate change on forest soil carbon: principles, factors, models, uncertainties. In: Freer-Smith P, Broadmeadow M, Lynch J, eds. Forestry and climate change. Wallingford: CAB International, 127–135.

Richter D deB, Billings SA. **2015**. 'One physical system': Tansley's ecosystem as Earth's critical zone. *New Phytologist* **206**: 900–912.

Rillig MC, Mummey DL. **2006**. Mycorrhizas and soil structure. *New Phytologist* **171**: 41–53.

Rineau F, Shah F, Smits MM, Persson P, Johansson T, Carleer R, Troein C, Tunlid A. **2013**. Carbon availability triggers the decomposition of plant litter and assimilation of nitrogen by an ectomycorrhizal fungus. *The ISME journal* **7**: 2010–2022.

Robinson D, Fitter AH. **1999**. The magnitude and control of carbon transfer between plants linked by a common mycorrhizal network. *Journal of Experimental Botany* **50**: 9–13.

Rosado S, Kropp B, Piché Y. **1994a**. Genetics of ectomycorrhizal symbiosis. I. Host plant variability and heritability of ectomycorrhizal and root traits. *New Phytologist* **126**: 105–110.

Rosado S, Kropp B, Piché Y. **1994b**. Genetics of ectomycorrhizal symbiosis II. Fungal variability and heritability of ectomycorrhizal traits. *New Phytologist* **126**: 111–117.

Ruess L, Chamberlain P. **2010**. The fat that matters: soil food web analysis using fatty acids and their carbon stable isotope signature. *Soil Biology and Biochemistry* **42**: 1898–1910.

Schielzeth H. **2010**. Simple means to improve the interpretability of regression coefficients. *Methods in Ecology and Evolution* **1**: 103–113.

Selosse MA, Richard F, He X, Simard SW. **2006**. Mycorrhizal networks: des liaisons dangereuses? *Trends in Ecology and Evolution* **21**: 621–628.

Semchenko M, Saar S, Lepik A. **2014**. Plant root exudates mediate neighbour recognition and trigger complex behavioural changes. *New Phytologist* **204**: 631–637.

Simard SW. **2009**. The foundational role of mycorrhizal networks in self-organization of interior Douglas-fir forests. *Forest Ecology and Management* **258**: 95–107.

Simard SW, Beiler KJ, Bingham MA, Deslippe JR, Philip LJ, Teste FP. **2012**. Mycorrhizal networks: Mechanisms, ecology and modelling. *Fungal Biology Reviews* **26**: 39–60.

Simard SW, Jones MD, Durall DM, Perry DA, David D, Molina R. **1997a**. Reciprocal transfer of carbon isotopes between ectomycorrhizal *Betula papyfera* and *Pseudotsuga menziesii*. *New Phytologist* **137**: 529–542.

Simard SW, Perry DA, Jones MD, Myrold DD, Durall DM, Molina R. **1997b**. Net transfer of carbon between ectomycorrhizal tree species in the field. *Nature* **388**: 579–582.

Söderström B. **1992**. The ecological potential of the ectomycorrhizal mycelium. In: Read D, Lewis D, Fitter A, Alexander IJ, eds. Mycorrhizal Functioning. Wallingford: CAB International, 77–83.

Soil Classification Working Group. **1998**. *The Canadian System of Soil Classification*. Ottawa.

Song YY, Simard SW, Carroll A, Mohn WW, Zheng RS. **2015**. Defoliation of interior Douglas-fir elicits carbon transfer and defense signalling to ponderosa pine neighbors through ectomycorrhizal networks. *Scientific Reports* **5**: 8495.

Song YY, Ye M, Li C, He X, Zhu-Salzman K, Wang RL, Su YJ, Luo SM, Zeng R Sen. **2014**. Hijacking common mycorrhizal networks for herbivore-induced defence signal transfer between tomato plants. *Scientific Reports* **4**: 3915.

Talbot JM, Allison SD, Treseder KK. **2008**. Decomposers in disguise: Mycorrhizal fungi as regulators of soil C dynamics in ecosystems under global change. *Functional Ecology* **22**: 955–963.

Teste FP, Karst J, Jones MD, Simard SW, Durall DM. **2006**. Methods to control ectomycorrhizal colonization: Effectiveness of chemical and physical barriers. *Mycorrhiza* **17**: 51–65.

Teste FP, Simard SW, Durall DM, Guy RD, Berch SM. **2010**. Net carbon transfer between *Pseudotsuga menziesii* var. *glauca* seedlings in the field is influenced by soil disturbance. *Journal of Ecology* **98**: 429–439.

Teste FP, Simard SW, Durall DM, Guy RD, Jones MD, Schoonmaker AL. **2009**. Access to mycorrhizal networks and roots of trees: importance for seedling survival and resource transfer. *Ecology* **90**: 2808–2822.

Verhoeven KJF, Simonsen KL, McIntyre LM. **2005**. Implementing false discovery rate control: increasing your power. *Oikos* **3**: 643–647.

Wallander H, Nilsson LO, Hagerberg D, Bååth E. **2001**. Estimation of the biomass and seasonal growth of external mycelium of ectomycorrhizal fungi in the field. *New Phytologist* **151**: 753–760.

White T, Bruns TD, Lee S, Taylor J. **1990**. Amplification and direct sequencing of fungal ribosomal RNA genes for phylogenetics. *PCR protocols: a guide to methods and applications* **18**: 315–322.

Wu B, Nara K, Hogetsu T. **2001**. Can ^{14}C-labeled photosynthetic products move between *Pinus densiflora* seedlings linked by ectomycorrhizal mycelia? *New Phytologist* **149**: 137–146.

Figure headings

Figure 1. Illustration of the plant and soil carbon pools sampled in each experimental unit, which consisted of (**a.**) one donor (D) and one full-sibling or unrelated recipient (R) *Pseudotsuga menziesii* var. *glauca* seedling in one pot separated by a nylon mesh bag (dark grey dashed cylinder) with holes of either 0.5 μm or 35 μm. In panels **b-f**, red and blue fill represents the donor and recipient pools, respectively. **b.** Above-ground plant biomass, divided into donor shoot pool (D_{shoot}) and recipient shoot pool (R_{shoot}). **c.** Below-ground plant biomass, divided into donor root pool (D_{root}) and recipient root pool (R_{root}). **d.** Below-ground plant-fungal biomass, divided into donor ectomycorrhizal root tip pool (D_{ECM}) and recipient ectomycorrhizal root tip pool (R_{ECM}). **e.** Soil attached to roots following their removal from soil and light shaking, divided into donor rhizosphere pool ($D_{rhizosphere}$) and recipient rhizosphere pool ($R_{rhizosphere}$); the donor rhizoplane pool ($D_{rhizoplane}$), very tightly adhering soil washed from root surface following vigorous vortexing in sterile water and subsequently pelleted by centrifugation, is approximated with solid black lines. **f.** Soil not attached to roots following their removal from soil and light shaking, divided into donor coarse soil pool (D_{coarse}) and recipient bulk soil pool (R_{bulk}).

Figure 2. Relatedness and hyphal restriction effects on *Pseudotsuga menziesii* var. *glauca* seedling R_{root} pool enrichment (excess ^{13}C as ^{12}C-equivalent), and their variation among recipient families. **a-b**, Standardised regression coefficients for linear mixed models (refer to Table 2), illustrating the differences between treatment levels in each recipient family in terms of their standardised effect size (SES). **a**. difference between kin and non-kin within mesh treatment (positive values indicate greater enrichment in kin pairs). **b**. difference between 35 μm and 0.5 μm mesh within relatedness treatment (positive values indicate greater enrichment in pairs separated by 35 μm mesh). Circles indicate average estimates, lines are 95% confidence intervals. Filled circles indicate significant difference between treatment levels, open points indicate no significant difference.

Figure 3. Linear regression of kin (left panels) and non-kin (right panels) ^{13}C-enrichment in *Pseudotsuga menziesii* var. *glauca* seedlings, revealing the positive relationships between: **a.** R_{root} $\delta^{13}C$ and D_{ECM} abundance (kin significant), **b.** R_{ECM} and D_{ECM} excess ^{13}C as ^{12}C-equivalent (mg) (kin significant), and **c.** R_{ECM} and D_{shoot} excess ^{13}C as ^{12}C-equivalent (mg) (kin significant). Circles represent data points. Black lines indicate significant linear relationship, grey lines indicate non-significant relationship. Note that kin and non-kin panels are scaled separately.

Figure 4. Incorporation of ^{13}C-label into PLFAs by different taxonomic groups in each biomass pool based on the average $\delta^{13}C$ of PLFAs. Error bars correspond to standard error. Dotted red line indicates natural abundance value of $\delta^{13}C$. Dashed vertical black line indicates separation

between donor and recipient pools by mesh bag. Text indicates whether biomass in the pool was primarily derived from plant material (*Pseudotsuga menziesii* var. *glauca*), plant and fungal material, the interface between plant/fungi and soil, or soil alone. PLFA identities are provided in Supporting Figures S2 and S3.

Table 1. Partitioning of plant-assimilated ^{13}C-labelled carbon in aboveground and belowground pools of interior Douglas-fir associated with ectomycorrhizal fungi six days after the start of a 10-h $^{13}CO_2$ labelling period

	^{13}C atom% excess (APE)	Total amount of excess ^{13}C (µg plant^{-1})						Excess ^{13}C incorporated of the mean total fixed (%)	
Pool	APE (s.e.m.)	Total µg (s.e.m.)	n	Kin µg (s.e.m.)	n	Non-kin µg (s.e.m.)	n	Kin % (s.e.m.)	Non-kin % (s.e.m.)
D_{shoot}	0.439 (0.037)	7050.67 (325.77)	35	6858.59 (521.51)	16	7212.41 (418.62)	19	31.345 (2.383)	32.962 (1.913)
D_{root}	0.238 (0.020)	1980.24 (159.76)	35	1878.00 (229.32)	17	2076.80 (226.67)	18	8.583 (1.048)	9.491 (1.036)
D_{ECM}	0.979 (0.068)	136.21 (27.57)	31	156.72 (56.54)	14	119.31 (20.52)	17	0.716 (0.258)	0.545 (0.094)
$D_{rhizoplane}$	0.076 (0.010)	231.81 (21.54)	36	241.61 (33.26)	17	223.04 (28.65)	19	1.104 (0.152)	1.019 (0.131)
$D_{rhizosphere}$	0.035 (0.004)	167.07 (20.08)	35	122.88 (22.96)	16	204.29 (29.39)	19	0.562 (0.105)	0.934 (0.134)
D_{coarse}	0.014 (0.002)	53.74 (11.29)	33	60.44 (18.81)	15	48.15 (13.69)	18	0.276 (0.086)	0.220 (0.063)
R_{bulk}	0.001 (0.000)	3.96 (0.50)	27	5.35 (0.83)	13	2.68 (0.39)	14	0.024 (0.004)	0.012 (0.002)
$R_{rhizosphere}$	0.004 (0.001)	4.90 (1.06)	33	4.80 (1.67)	16	4.98 (1.39)	19	0.022 (0.008)	0.023 (0.006)
R_{ECM}	0.119 (0.021)	2.43 (0.48)	34	2.48 (0.86)	16	2.39 (0.52)	18	0.011 (0.004)	0.011 (0.002)
R_{root}	0.013 (0.001)	3.76 (0.47)	33	4.96 (0.80)	16	2.64 (0.35)	17	0.023 (0.004)	0.012 (0.002)
R_{shoot}	0.006 (0.001)	2.76 (1.11)	6	3.46 (1.59)	4	1.37 (0.59)	2	0.016 (0.007)	0.006 (0.003)
Plant and soil mean values									
D_{plant}		9167.11		8893.31		9408.52		40.64	43.00
D_{soil}		452.62		424.93		475.48		1.94	2.17
R_{soil}		8.86		10.15		7.66		0.05	0.03
R_{plant}		8.95		10.89		6.40		0.05	0.03

APE = atom percent excess; n = number of significantly enriched samples; Total amount added during pulse = 29 020 µg excess ^{13}C; Mean amount fixed after 1-day chase = 21 881.08 µg excess ^{13}C

766 **Table 2.** Effects of hyphal restriction and donor relatedness treatments on excess ^{13}C as ^{12}C equivalent (μg) of recipient *Pseudotsuga menziesii*
767 var. *glauca* seedling biomass pools, using maximum likelihood analysis of linear mixed-effects models[1] and likelihood ratio tests

Pool	**R_{bulk}**			**$R_{rhizosphere}$**			**R_{ECM}**			**R_{root}**		
Data transformation	-			sqrt			-			log_{10}		
Marginal R^2	0.605			0.565			0.325			0.673		
Factor	**df**	***F*-value**	***P*-value**	**df**	***F*-value**	***P*-value**	**df**	***F*-value**	***P*-value**	**df**	***F*-value**	***P*-value**
Intercept	1,15	**97.53**	**<0.0001**	1,15	**283.15**	**<0.0001**	1,15	**50.41**	**<0.0001**	1,15	**110.65**	**<0.0001**
Relatedness (Re)	1,15	1.81	0.199	1,15	0.15	0.708	1,15	0.08	0.787	1,15	**6.47**	**0.020**
Hyphal (Hy)	1,15	3.65	0.077	1,15	3.29	0.090	1,15	0.79	0.387	1,15	**5.38**	**0.032**
Recipient Family (Rfam)	3,15	2.79	0.079	3,15	2.14	0.138	3,15	0.31	0.816	3,15	0.50	0.687
Re*Hy	1,15	0.14	0.710	1,15	0.31	0.585	1,15	1.82	0.197	1,15	2.34	0.143
Re*Rfam	3,15	0.37	0.775	3,15	0.61	0.619	3,15	1.55	0.243	3,15	**4.59**	**0.015**
Hy*Rfam	3,15	**3.36**	**0.050**	3,15	**3.54**	**0.041**	3,15	0.03	0.991	3,15	**4.14**	**0.021**

768 Values in bold are significant at the $\alpha < 0.05$ level.

769 Marginal R^2 = model fit based on fixed factors alone. Inclusion of random factor did not increase model fit.

770 [1]Model form: (Pool) ~ (Re)*(Hy) + (Re)*(Rfam) + (Hy)*(Rfam), random ~ 1| (Donor family)

771 **Table 3.** Identity and relative abundance of root-associated fungi on kin and non-kin *Pseudotsuga menziesii* var. *glauca* seedlings based on root
772 tip morphotyping and ITS region taxonomic classification. No significant differences in colonisation were observed between mesh sizes.

Fungal morphotype ID	Seedling	Relative abundance		Accession	Sequence match (NCBI accession)	% Identity
		Kin	Non-kin			
Rhizopogon vinicolor (Morphotype 1)	Donor	0.46	0.58	KT314836	*Rhizopogon vinicolor* (AF263933)	652/656 (99%)
	Recipient	0.44	0.57			
Rhizopogon vinicolor (Morphotype 2)	Donor	0.24	0.11	KT314840	*Rhizopogon vinicolor* (HQ385848)	529/535 (99%)
	Recipient	0.14	0.03			
Pyronemataceae sp.	Donor	0.12	0.09	KT314854	uncultured Pyronemataceae (GU452518)	524/524 (100%)
	Recipient	0.26	0.29			
Wilcoxina sp.	Donor	0.08	0.05	-	Sequencing failed – Taxonomic ID	-
	Recipient	0.13	0.09			
Uncolonised root tips	Donor	0.05	0.15	N/A	N/A	N/A
	Recipient	0.00	<0.01			
Fusarium sp.	Donor	0.03	0.01	KT314859	*Fusarium acuminatum* (KP068924)	478/478 (100%)
	Recipient	0.03	0.02	KT314860	*Fusarium oxysporum* (KP132221)	451/451 (100%)
Rhizopogon sp.	Donor	0.01	0.01	KT314850	*Rhizopogon fragrans* (AM085523)	619/621 (99%)
	Recipient	< 0.01	< 0.01			
Rhizopogon ochraceisporus	Donor	0.01	0.00	KT314851	*Rhizopogon ochraceisporus* (AF366389)	603/609 (99%)
	Recipient	0.00	0.00			

773 N/A = not applicable (uncolonised root tips which did not generate fungal DNA).
774

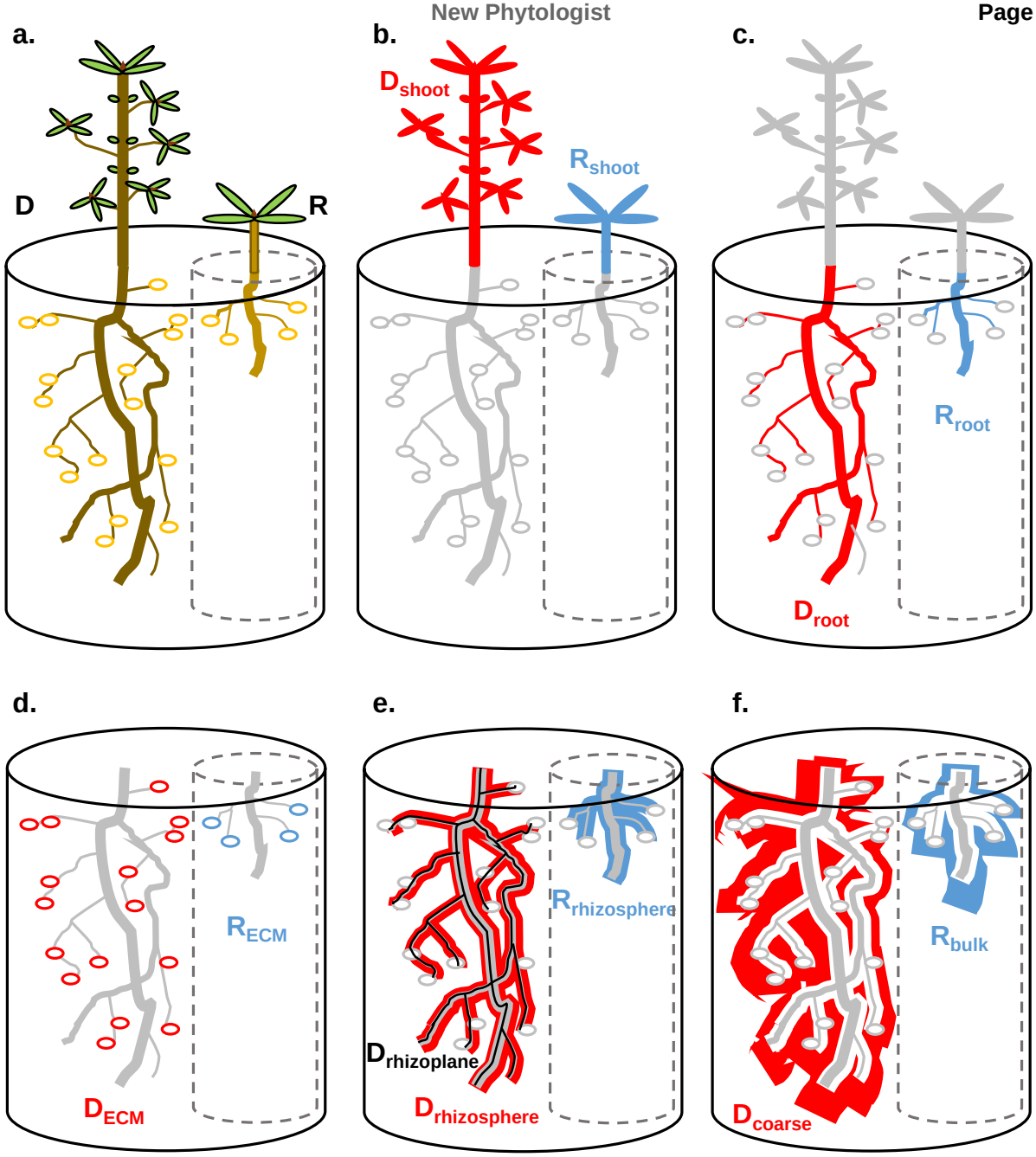
a.
D
R
b.
D shoot
R shoot
c.
R root
D root
d.
R ECM
D ECM
e.
R rhizosphere
D rhizoplane
D rhizosphere
f.
R bulk
D coarse

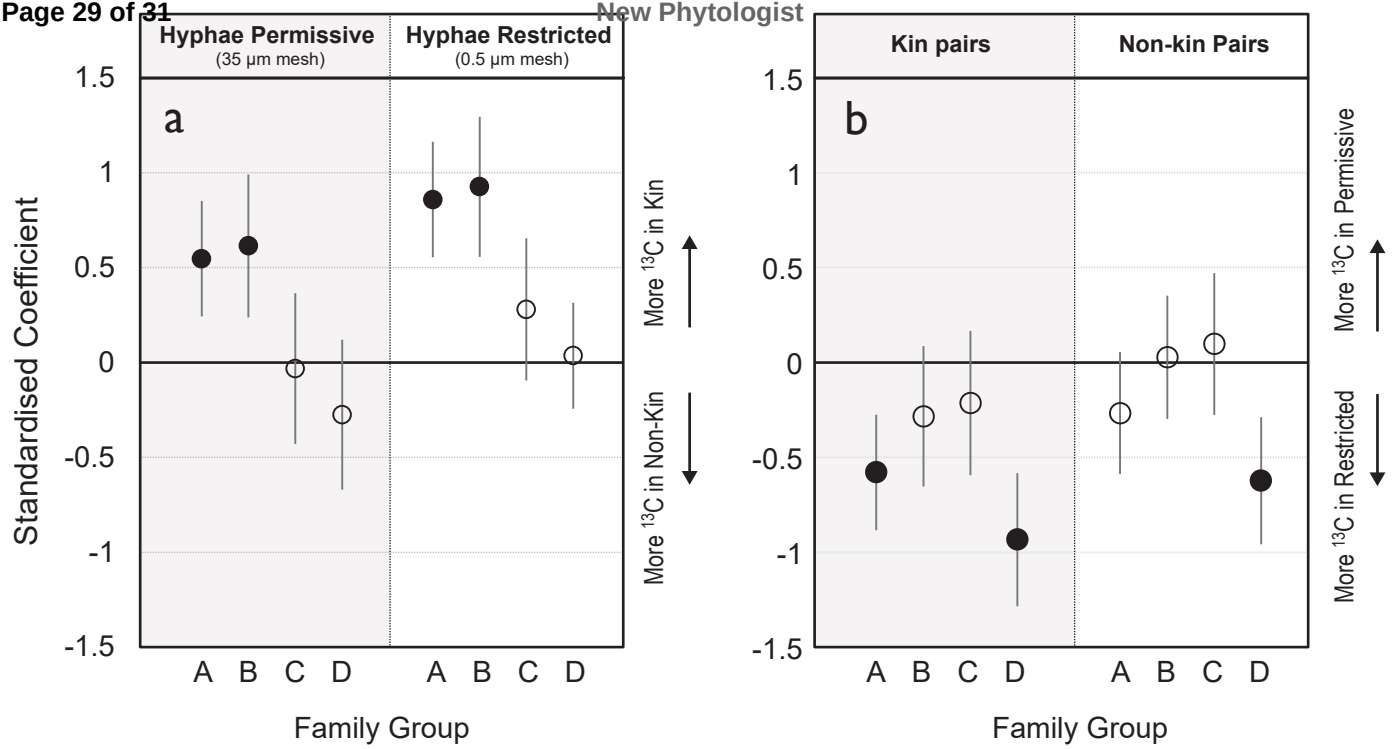
Hyphae Permissive
(35 µm mesh)
Hyphae Restricted
(0.5 µm mesh)
a
b
Kin pairs
Non-kin Pairs
Standardised Coefficient
1.5
1
0.5
0
-0.5
-1
-1.5
A B C D A B C D
Family Group
More 13C in Kin
More 13C in Non-Kin
More 13C in Permissive
More 13C in Restricted

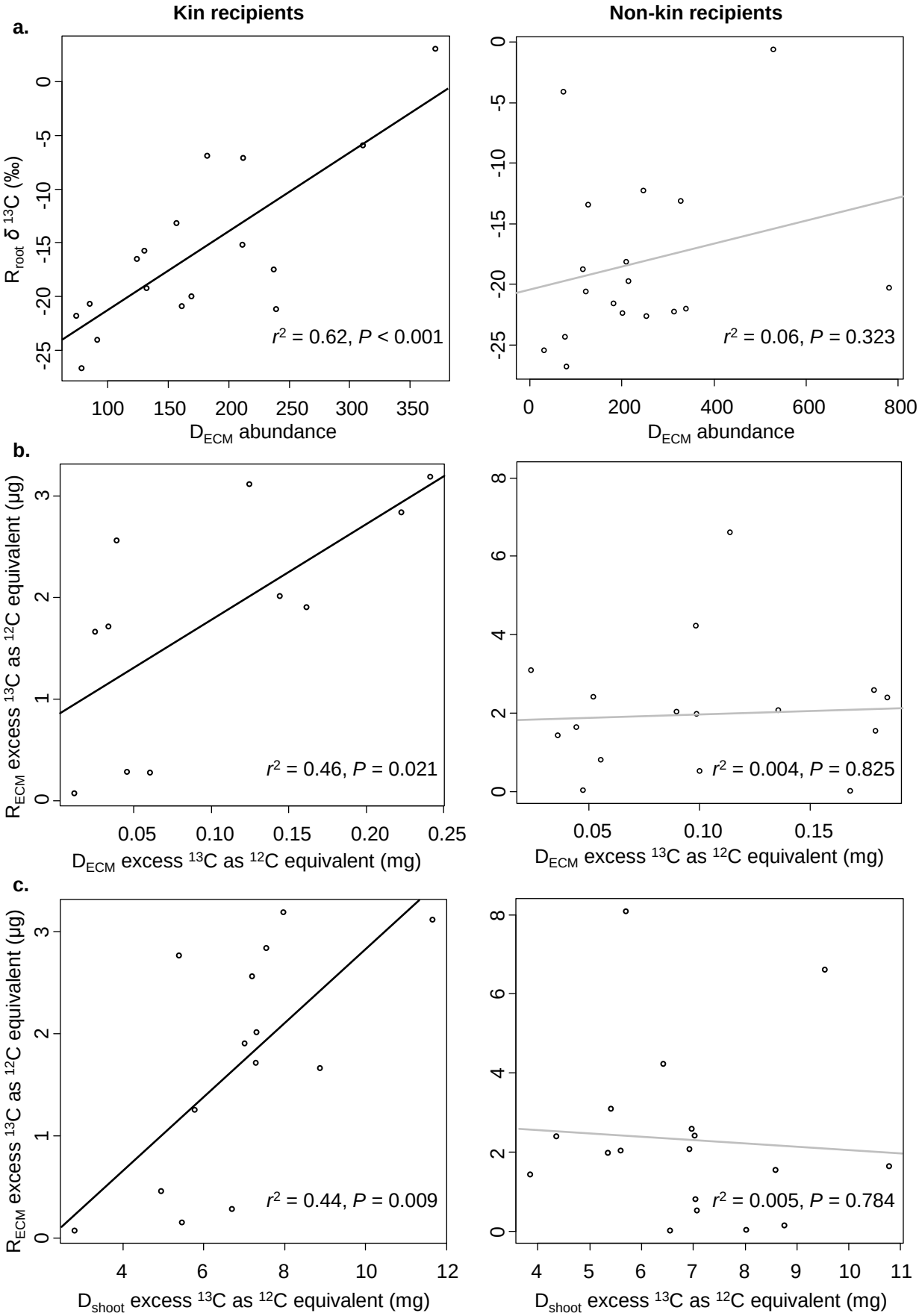
Kin recipients
Non-kin recipients
a.
R_{root} δ ^{13}C (‰)
D_{ECM} abundance
r^2 = 0.62, P < 0.001
r^2 = 0.06, P = 0.323
b.
R_{ECM} excess ^{13}C as ^{12}C equivalent (µg)
D_{ECM} excess ^{13}C as ^{12}C equivalent (mg)
r^2 = 0.46, P = 0.021
r^2 = 0.004, P = 0.825
c.
R_{ECM} excess ^{13}C as ^{12}C equivalent (µg)
D_{shoot} excess ^{13}C as ^{12}C equivalent (mg)
r^2 = 0.44, P = 0.009
r^2 = 0.005, P = 0.784

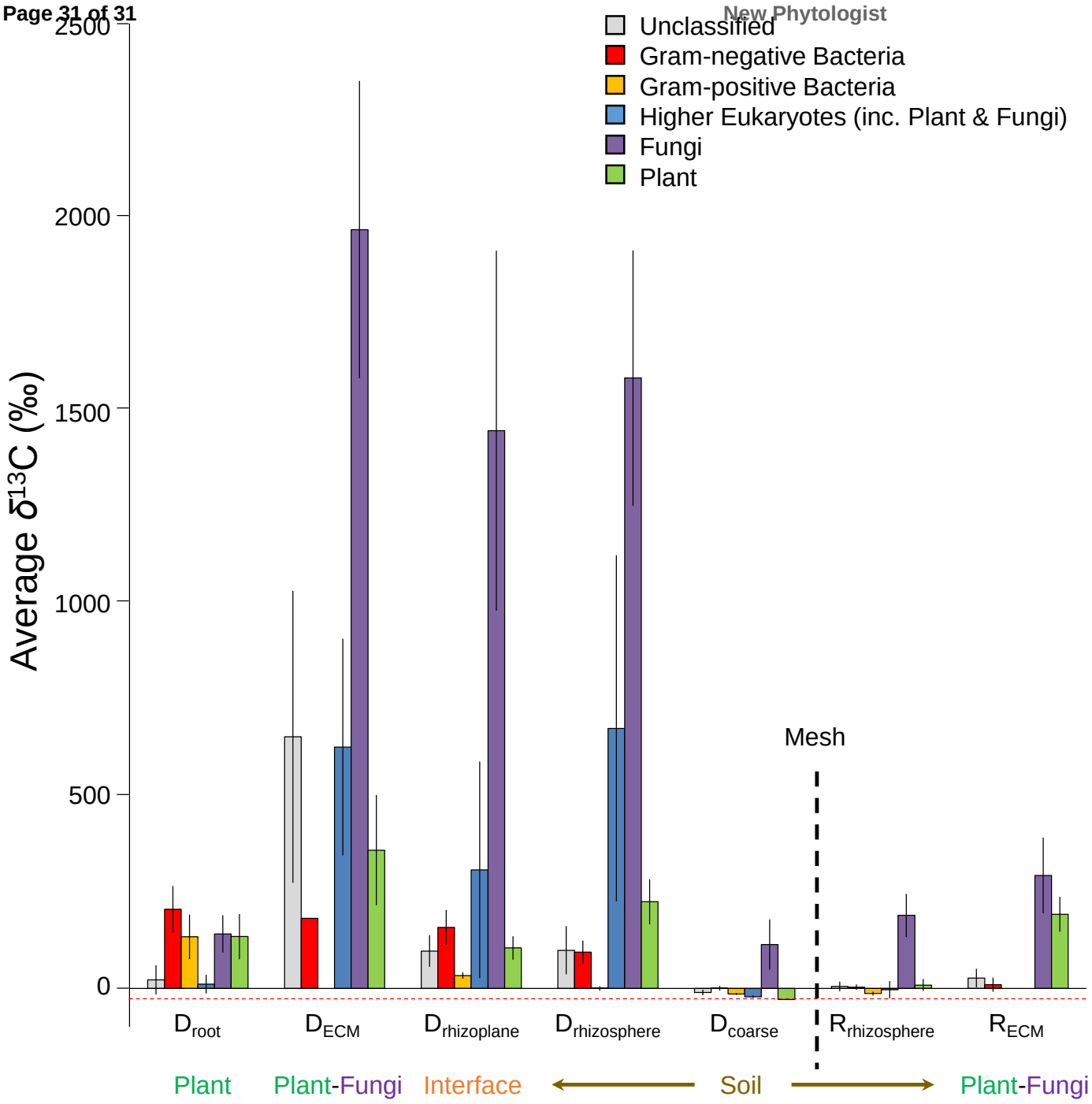
Unclassified
Gram-negative Bacteria
Gram-positive Bacteria
Higher Eukaryotes (inc. Plant & Fungi)
Fungi
Plant
Average δ13C (‰)
2500
2000
1500
1000
500
0
Mesh
Droot
DECM
Drhizoplane
Drhizosphere
Dcoarse
Rrhizosphere
RECM
Plant
Plant-Fungi
Interface
Soil
Plant-Fungi